TPR-97-05

Manifestation of Classical Orbits in Nuclei, Metal Clusters and Quantum Dots

M. Brack[a], P. Meier[a], S. M. Reimann[b], M. Sieber[c]

[a] *Institut für Theoret. Physik, Universität, D-93040 Regensburg, Germany*
[b] *Niels Bohr Institutet, Blegdamsvej 17, DK-2100 Copenhagen Ø, Denmark*
[c] *Abteilung Theoretische Physik, Universität Ulm, D-89069 Ulm, Germany*

Abstract. We first give a short outline of the semiclassical periodic orbit theory that allows one to relate quantum shell fluctuations in a mean-field system to the periodic orbits of the corresponding classical system. Earlier applications to gross-shell effects in nuclei (ground-state deformations), metal clusters (ground-state deformations and supershells), and quantum dots (conductance oscillations in weak magnetic fields) are briefly summarized. We then report on a recent simple and transparent semiclassical interpretation of the origin of the mass asymmetry in the fission of heavy nuclei. Using only a few classical periodic orbits and a cavity model for the nuclear mean field, we explain the onset of left-right asymmetric shapes at the fission isomer minimum by the principle of constant action of the shortest orbits.

1. ROLE OF PERIODIC ORBITS IN FINITE FERMION SYSTEMS

Almost three decades ago, Gutzwiller derived a semiclassical theory that culminated 1971 in the so-called 'trace formula' [1]. It expresses the oscillating part $\delta g\,(E)$ of the density of states of a quantum system by a sum over all periodic orbits of the corresponding classical system, assuming that these orbits be isolated in phase space. Shortly thereafter, Balian and Bloch presented a corresponding expression for the density of eigenstates of a three-dimensional cavity of arbitrary shape with ideally reflecting walls [2]; their derivation is valid also for systems with continuous symmetries and the families of degenerate periodic orbits occurring therein. Strutinsky, Magner and coworkers subsequently extended Gutzwiller's theory to incorporate degenerate orbit families and applied it successfully to potentials with continuous symmetries [3].

In all these and later versions of the semiclassical 'periodic orbit theory' (POT), the basic form of the trace formula is the same:

$$\delta g\,(E) \simeq \Re e \sum_{po} \mathcal{A}_{po}(E) \exp\left\{ i \left[\frac{1}{\hbar} S_{po}(E) - \sigma_{po} \frac{\pi}{2} \right] \right\}. \qquad (1)$$

The sum is taken over all periodic orbits, labeled '*po*', of the classical system. S_{po} are the action integrals along the periodic orbits and σ_{po} are phases related to the number of conjugate points along the orbits. The amplitude $\mathcal{A}_{po}$ of each orbit depends on its period, its stability and its degeneracy. Together with the smooth level density $\widetilde{g}\,(E)$, which can be obtained in the (extended) Thomas-Fermi model, Eq. (1) approximates the exact quantum-mechanical level density:

$$\widetilde{g}\,(E) + \delta g\,(E) \simeq g\,(E) = \sum_i \delta(E - E_i)\,, \tag{2}$$

where E_i are the eigenenergies of the system and the sum runs over all quantum states i. An introduction to the POT and detailed explanations of all the above ingredients may be found in Ref. [4].

Gutzwiller's original trace formula for isolated orbits [1] has been used to study the semiclassical quantization of chaotic systems [5]. A different use of the POT [3, 4] is to obtain a coarse-grained level density by keeping only the shortest orbits with the largest amplitudes in the trace formula (1). This allows one to relate the gross-shell structure of interacting fermion systems in the mean-field approximation to a few classical orbits. For such systems it is useful to write the total energy in the form

$$E_{tot} = \widetilde{E} + \delta E\,, \tag{3}$$

where $\widetilde{E}$ is the average total energy of the interacting system and δE is its oscillating part, the so-called 'shell-correction energy' which quantum mechanically is obtained, according to Strutinsky [6], in terms of the single-particle energies E_i of the selfconsistent mean field. Using Eq. (1), the semiclassical expression for the energy shell correction δE becomes [3, 4]

$$\delta E \simeq \sum_{po} \delta E_{po} = \Re e \sum_{po} \mathcal{A}_{po}(E_F) \left(\frac{\hbar}{T_{po}}\right)^2 \exp\left\{i\left[\frac{1}{\hbar} S_{po}(E_F) - \sigma_{po}\frac{\pi}{2}\right]\right\}. \tag{4}$$

Here E_F is the Fermi energy and $T_{po} = dS_{po}/dE|_{E_F}$ the period of the orbit labeled *po*.

Including only the shortest and most degenerate orbits in Eq. (4) is often sufficient to explain gross-shell effects in the total energy of a mean-field system. Pioneering work in this direction has been done by Strutinsky *et al.* [3], who gave a semiclassical explanation of the systematics of nuclear ground-state deformations. They showed that the ground-state minima of the nuclei as functions of particle number and deformation are correctly reproduced by the condition that the action of the dominating family of periodic orbits be stationary. Their treatment was extended by Frisk [7]. The same analysis also allowed for a semiclassical interpretation of microscopically calculated ground-state deformations of large spheroidal metal clusters [8].

Another beautiful example is the beating pattern of the coarse-grained level density in a spherical cavity, which by Balian and Bloch [2] was related

to the interference of the triangular and square periodic orbits. Its occurrence in metal clusters in the form of the so-called 'supershells' has later been predicted by Nishioka *et al.* [9] and observed experimentally for the first time by Pedersen *et al.* [10]. The experimental sequence of magic numbers $N_i \geq 58$ in simple metal clusters, which correspond to filled spherical shells of the valence electrons, are quantitatively reproduced in this semiclassical picture by the average length of the triangle and square orbits, even using the simple spherical cavity model [9, 11]. The difference of their orbit lengths gives approximately the correct length of the supershell beat which, however, depends also on the details of the potential surface and on contributions from longer orbits [9, 12].

Finally, we mention the recent experimental observation [13] of conductance oscillations in a large circular quantum dot with a perpendicular weak magnetic field B. An analysis of the results in terms of periodic orbits in a circular billiard was given in Ref. [14]. The period of the oscillations versus the dot radius is correctly given by the average length of the two leading orbits, which here are the diameter and the triangle orbits, whereas the period of the B-field oscillation is well explained by the magnetic flux through the shortest orbit enclosing a nonzero area, i.e., the triangle orbit.

For the remainder of this paper, we shall discuss and extend a very recent application [15] of the POT to an old topic in nuclear physics: the left-right asymmetry of nuclear fission.

2. A SIMPLE EXPLANATION OF THE MASS ASYMMETRY IN NUCLEAR FISSION

A well-known feature of the fission of many actinide nuclei is the asymmetric mass distribution of the fission fragments. The liquid drop model [16] correctly describes many aspects of the fission process qualitatively, but cannot explain the mass asymmetry in heavy nuclei where the fissility parameter x is close to unity [17]. The asymmetry is a quantum shell effect coming from the discrete spectra of the nucleons in their mean fields. It was correctly described by Strutinsky's shell-correction method [6] which accounts for the shell effects in the nuclear energy. One writes the total energy of a nucleus consisting of N neutrons and Z protons as

$$E_{tot}(N,Z;def) = E_{LDM}(N,Z;def) + \delta E_n(N;def) + \delta E_p(Z;def)\,, \qquad (5)$$

where E_{LDM} is the liquid drop model (LDM) energy and δE_n, δE_p are the shell-correction energies of the neutrons and protons, respectively, which are obtained from the single-particle spectra of realistic shell-model potentials. All quantities above depend on the shape of the nucleus which must be described by some suitable deformation parameters; these are summarized here by 'def'. The shell-correction approach, which is formally based [6, 18] on

the Hartree-Fock theory [19], was very successful in reproducing experimental nuclear binding energies and fission barriers [18, 20, 21].

The shell effects in the total energy (5) of a typical actinide nucleus lead to a deformed ground-state minimum and to a higher-lying local minimum, the so-called fission isomer. The fission barrier therefore exhibits a characteristic double-humped structure [22]. When left-right asymmetric nuclear shapes are included in the calculation, the total energy is found [23, 24] to be lowered along the way over the outer barrier, starting at the fission isomer. The gain in energy persists all the way down towards the scission point where the nucleus breaks into two fragments of unequal size. (The axial symmetry is preserved in the whole region beyond the inner barrier [25].) It is important to note that the onset of the mass asymmetry takes place already at an early stage of the fission process, long before the nucleus breaks up. It is a pure quantum effect which only comes about if the shell corrections are included into the total energy (5). Of course, a dynamical theory involving inertial parameters is required to predict the detailed mass distributions of the fission fragments [26]. But, interestingly enough, the most probable experimental mass ratios are roughly those of the nascent fragments found statically at the asymmetric outer barrier.

In the following we give a very simple and transparent semiclassical interpretation of this static quantum effect. For simplicity, we replace the nuclear mean field by a cavity with reflecting walls, neglect the spin-orbit interaction, and consider only one kind of particles. This yields the main physical effects, since the neutron contribution δE_n to the total energy contains the largest shell effects [18]. We employ the parameterization (c, h, α) of Ref. [18] to define the boundary of the cavity [in cylindrical coordinates (ρ, z, ϕ), with the symmetry axis along z] by the shape function $\rho = \rho(z; c, h, \alpha)$. Here c is the length of the semiaxis in the z direction in units of the radius R_0 of the spherical cavity (c=1, h=α=0). The parameter h regulates the formation of a neck leading to the scission of the nucleus into two fragments, and $\alpha \neq 0$ yields left-right asymmetric shapes. The volume of the cavity is kept constant for all deformations. The parameters (c, h) are chosen such that the one-dimensional curve $E_{LDM}(c)$ along h=α=0 follows the adiabatic fission barrier of the LDM. When the shell effects are included, $E_{tot}(c, \alpha)$ along h=0 gives already a realistic two-dimensional picture of the asymmetric outer fission barrier in actinide nuclei.

We now have to determine the shortest periodic orbits of this system to calculate the gross-shell structure in δE. At large deformations (here $c \gtrsim 1.4$), these are known [7, 27] to be the orbits lying in equatorial planes perpendicular to the symmetry axis. The positions z_i of these planes along the z axis are given by the condition $d\rho(z; c, h, \alpha)/dz|_{z_i} = 0$. The periodic orbits are regular polygons [2] characterized by (p, t), where p is the number of reflections at the boundary and t the number of windings around the z

axis ($p \geq 2$, $t \leq p/2$). The lengths of the orbits are $L_{pt}^{(i)} = 2pR_i \sin(\pi t/p)$, where $R_i = \rho(z_i; c, h, \alpha)$, and their actions are $S_{pt}^{(i)}(E_F) = \hbar k_F L_{pt}^{(i)}$ in terms of the Fermi wave number $k_F = \sqrt{2mE_F}/\hbar$. The contribution of these orbits to Eq. (1) has been derived by Balian and Bloch [2]; we refer to their paper for the explicit form of the amplitudes $\mathcal{A}_{pt}$ and phases σ_{pt}.

The trace formulae (1) and (4) with these amplitudes are, however, only meaningful as long as the orbits are well separated from neighboring periodic orbits, in particular only as long as the orbits are sufficiently far from bifurcations. Yet in systems which are neither completely chaotic nor integrable it is typical that periodic orbits bifurcate when a parameter of the system is varied. At a bifurcation, two or more periodic orbits coincide, their amplitudes A_{pt} diverge, and the trace formula has to be modified. For the present investigations we need consider only one type of bifurcation. It occurs when the positions z_i of different equatorial planes coincide. In the (c, h, α) parameterization, there are at most three such planes. One plane exists always; the other two arise at the points (c_0, h_0, α_0) where the neck formation starts. In the symmetric case (α=0), one plane is always located at z_0=0 and, beyond the bifurcation point, the other two are located symmetrically at $\pm z_1$ (with $z_1 > 0$) and contain identical periodic orbits.

Near a bifurcation point, all orbits of type (p, t) from the neighboring planes give a joint contribution to $\delta g\,(E)$ and δE that can be derived from a multiple reflection expansion of the Green's function [2], yielding the integral

$$\delta E_{pt} = \Re e \int_{-c}^{+c} dz\, f_{pt}(z) \exp\{ik_F L_{pt}(z)\}\,, \tag{6}$$

where $f_{pt}(z)$ is a slowly varying analytic function of z. Since the plane positions z_i of the periodic orbits are determined by the stationary points of the length function $L_{pt}(z) = 2p \sin(\pi t/p)\rho(z; c, h, \alpha)$, a stationary phase evaluation of (6) leads back to separate contributions to Eq. (4) for each plane, with the amplitudes and phases given in [2]. In order to obtain an approximation to (6) that is valid at the bifurcation as well as far from it, we employ a uniform approximation appropriate for the case of three nearly coincident stationary points in a one-dimensional oscillatory integral [28]. We obtain

$$\delta E_{pt} = \Re e \left\{ [u_4 P(u_1, u_2) + u_5 P_x(u_1, u_2) + u_6 P_y(u_1, u_2)]\, e^{iu_3} \right\}\,, \tag{7}$$

where $P(x, y)$ denotes Pearcey's integral defined by

$$P(x, y) = \int_{-\infty}^{\infty} dz\, \exp[\, i(z^4 + xz^2 + yz)]\,, \tag{8}$$

and $P_x(x, y)$, $P_y(x, y)$ are its derivatives with respect to the first and second argument, respectively. The constants $u_1 \ldots u_6$ are determined by the semiclassical amplitudes, actions and phases of the periodic orbits. If the

orbits are well separated, Eq. (7) reduces to the standard contributions of type (p,t) to the trace formula (4). In the symmetric case (α=0), the result (7) can be simplified and yields a formula which is analogous to that for a generic pitchfork bifurcation [29] and can be given analytically [15]. Also in the strongly asymmetric case, the result (7) can be simplified when the contribution of one orbit plane can be considered separately from that of the other two orbit planes arising at the point where the neck formation starts. In the general case, however, the entire Pearcey integral and its derivatives have to be used and evaluated numerically.

Before we discuss the fission barriers obtained [15] in the semiclassical approximation using Eq. (7), we present here some tests of the accuracy of the semiclassical theory by comparing its results with those of exact quantum-mechanical calculations using the same cavity model.

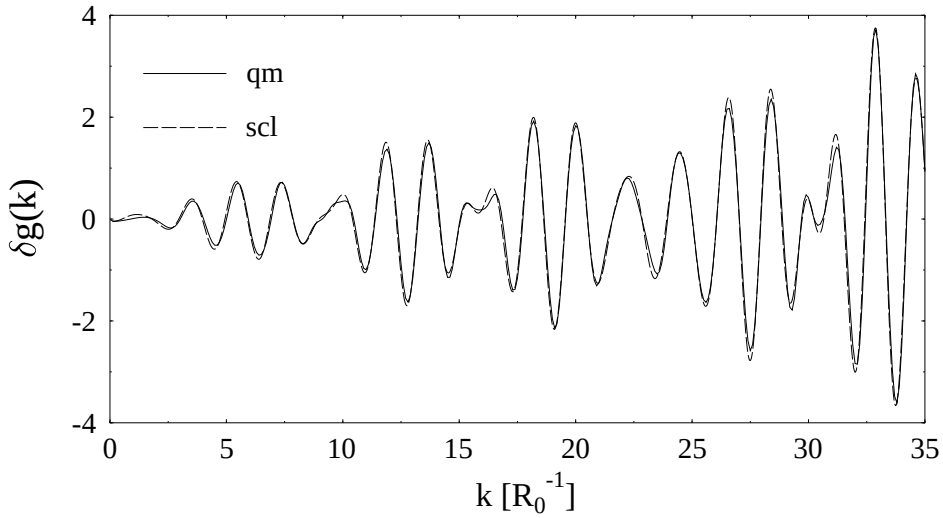

Figure 1: Oscillating part of the level density at a bifurcation point (c=1.498, h=0, α=0). Quantum-mechanical (solid line) and semiclassical results (dashed line), averaged over the wave number k by a Gaussian of width γ=0.6/R_0. Only orbits with t=1 and $p \leq 10$ are included in the semiclassical case.

In Fig. 1 we compare the oscillating part $\delta g\,(k)$ of the level density, calculated quantum-mechanically (solid line) and semiclassically in the uniform approximation (dashed line), as a function of the wave number k. The deformation has been chosen to correspond to a bifurcation point (c=1.498, h=0, α=0) close to the symmetric outer fission barrier (see below), at which the standard Gutzwiller (or Balian-Bloch) trace formula diverges. Both results have been averaged over k by a Gaussian of width γ=0.6/R_0, in order to emphasize the gross-shell effects with a resolution typical of that obtained with the shell-correction method. In the semiclassical calculation, only orbits with t=1 and $p \lesssim 6$ contribute within the numerical accuracy of the figure.

We see that with a small number of periodic orbits, the present semiclassical theory reproduces the coarse-grained quantum level density quantitatively.

Another test of the semiclassical approximation is shown in Fig. 2, where we compare the Fourier transforms of the quantum and semiclassical results for $\delta g\,(k)$, this time chosen at a left-right asymmetric deformation corresponding to the point B in the deformation energy surfaces shown in Figs. 3 and 5 below. Taking the Fourier transform of $\delta g\,(k)$ with respect to the wave number k yields directly the length spectrum of the classical periodic orbits.

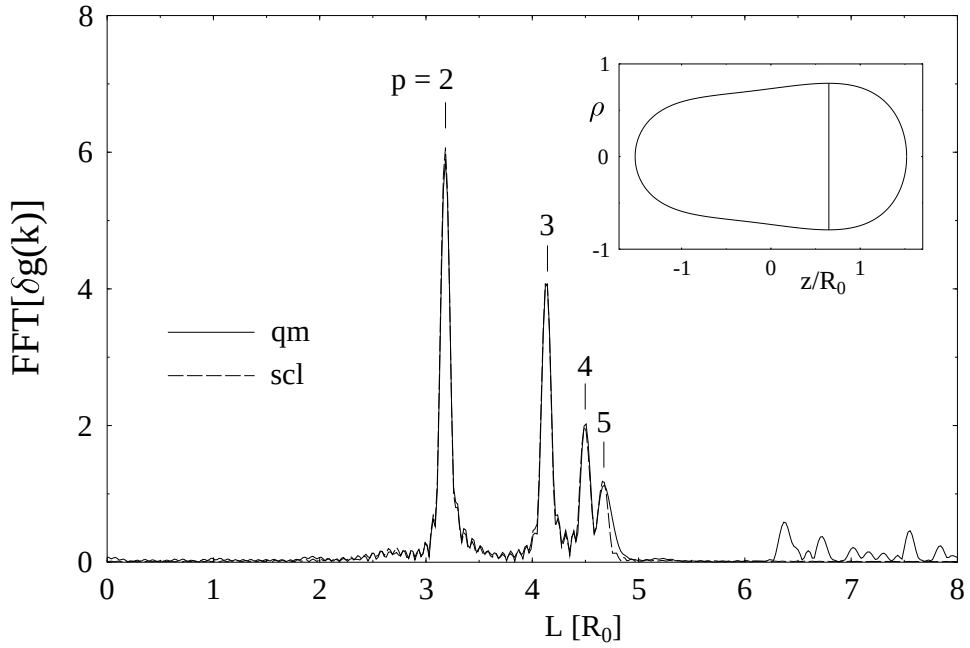

Figure 2: Squared amplitudes of the Fourier transforms of $\delta g(k)$ (averaged as in Fig. 1), obtained quantum mechanically (solid line) and semiclassically using only t=1 (dashed line). An asymmetric deformation (c=1.5, h=0, α=0.12) was chosen which corresponds to the point B shown on Figs. 3 and 5 below. The insert on the upper right shows the shape of the cavity and the location of the equatorial plane that contains the periodic orbits with reflection number p.

We clearly see in Fig. 2 the peaks corresponding to the diameter (p=2) and the polygons with $p = 3$, 4, and 5 corners, all with winding number t=1. The contributions from $p \geq 6$ are negligible for the chosen width (γ=0.6/R_0 as in Fig. 1). The peak heights are quantitatively reproduced by the semiclassical result. In the spectrum of the quantum-mechanical level density, a slight indication of the second repetition of the diameter orbit (p, t)=(4,2) can be seen at $L \simeq 6.3\,R_0$; it hardly exceeds, however, the numerical noise. We can therefore trust the semiclassical approximation and, within the present coarse-graining of the shell structure, the restriction to orbits with t=1.

Encouraged by the positive results of these tests, we now proceed to calculate the total contribution of all equatorial orbits with t=1 to the shell-correction energy δE, given by Eq. (7) and summing over p. (No Gaussian averaging has been done for δE.) In the right-hand panels of Fig. 3 we show contour plots of the δE in the (c, α) plane for two values of the neck parameter. The energy unit is $E_0 = \hbar^2/2mR_0^2$. The Fermi wave number was chosen to be $k_F = 12.1/R_0$, such that δE has a minimum at the correct deformation c =1.42, h=α=0 of the fission isomer [18]. Only orbits with winding number one (t=1) and with up to $p_{max} = 10$ reflections were included. The results actually remain the same within a few percent when only orbits with $p = 2$ and 3, i.e., only diameter and triangle orbits are included. (Even with the diameter alone, one obtains already the same topology of the deformation energy surface.)

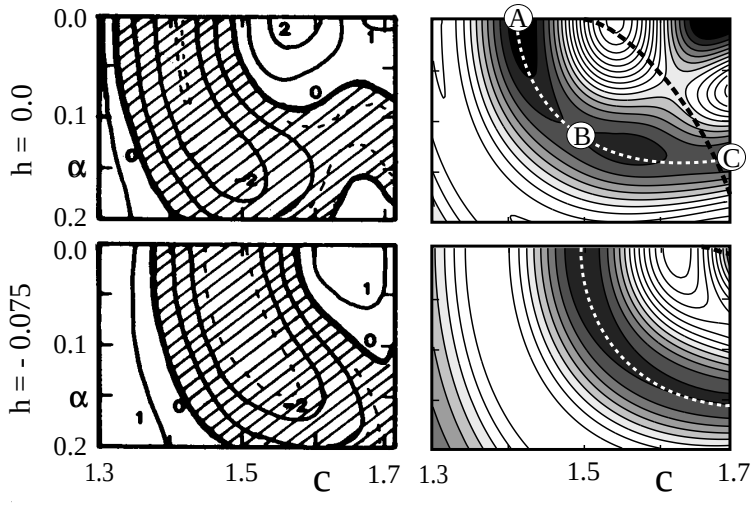

Figure 3: Contour plots of deformation energy versus elongation c and asymmetry α for two values of the neck parameter: h=0 (above) and h=−0.075 (below). *Left side*: quantum-mechanical neutron shell-correction energy of ^{240}Pu from Ref. [18]. *Right side*: semiclassical shell-correction energy δE. White dashed lines follow the loci of constant classical actions of the leading equatorial periodic orbits; black dashed lines follow the loci of the bifurcation points.

On the left of Fig. 3 we have reproduced the neutron shell-correction energy δE_n of the nucleus ^{240}Pu, obtained in Ref. [18] with a realistic Woods-Saxon type shell-model potential. Note that in these results, short-range pairing correlations are included that lead to a smoothing of the level spectrum around the Fermi energy. This causes, in the language of the POT, a suppression of longer periodic orbits. Furthermore, the amplitudes in the trace formula (4) for δE are divided by their squared periods T_{po}, which additionally damps the contributions of longer orbits. For these reasons,

the equatorial orbits with winding numbers $t > 1$ as well as other longer orbits – such as the diameter along the symmetry axis (which is isolated) and polygons lying in planes containing the symmetry axis [3] – will not change the semiclassical results significantly within the given resolution of the shell structure in δE. The rapid convergence of the contributions of t=1 orbits with increasing number p of corners, whose lengths saturate at $2\pi R_i$, is demonstrated in Fig. 4. Here we show δE versus the asymmetry parameter α at the deformation c=1.53, h=0, corresponding to the top of the symmetric barrier at α=0, for increasing maximum values of p.

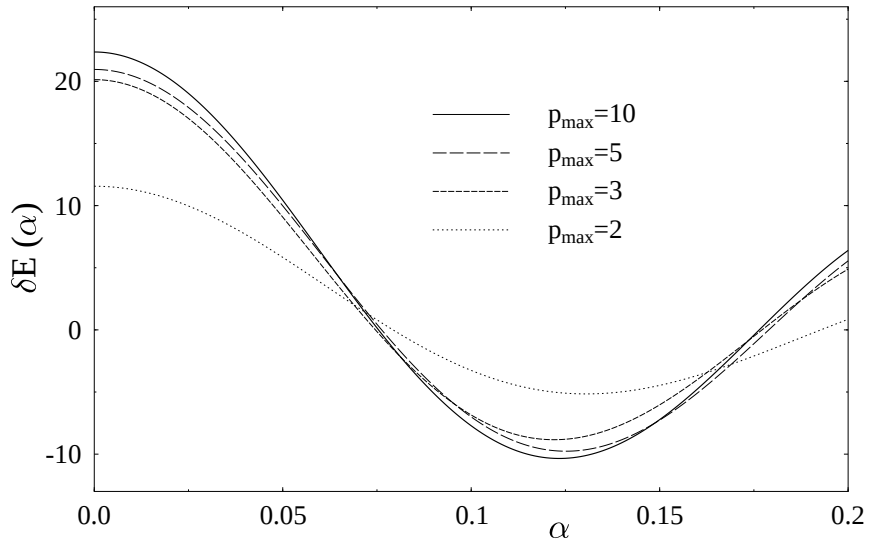

Figure 4: Convergence of the semiclassical energy shell-correction δE, plotted versus the asymmetry parameter α, for increasing maximum number p_{max} of corners of the included equatorial orbits (t=1). (Deformation: c=1.53, h=0.)

At this point we would like to mention that Arita and Matsuyanagi [30] have studied the effect of left-right asymmetric deformations of octupole type on the supershell structure in harmonic-oscillator potentials and discussed them in terms of periodic orbits. They pointed out that the second repetitions of the shortest orbits in this system undergo bifurcations which tend to enhance the shell effects connected to the octupole deformations near the bifurcation points. More recently, Sugita *et al.* [31] did the same analysis also in superdeformed spheroidal cavities with axis ratio 2 and additional octupole deformations, observing the same effects. Both these systems (harmonic oscillators and spheroidal cavities) have an additional continuous symmetry besides the axial one, such that the new three-dimensional orbits born at the bifurcations occur in doubly-degenerate families and hence have enhanced semiclassical amplitudes. However, the cavities which we are investigating here do not have such an extra symmetry because of their rather strong

hexadecapole deformations. As a consequence, bifurcations of the second repetitions (t=2) of the equatorial orbits are not expected to play an important role for the gross-shell effects in the present system.

We see from Fig. 3 that the semiclassical result even in the simplified cavity potential correctly reproduces the topology of the deformation energy in the (c, α) plane and, in particular, the onset of the mass asymmetry at the fission isomer; this holds for both values of h. The loci of the bifurcation points (c_0, α_0) at which the number of equatorial orbit planes bifurcates from one to three are indicated in Fig. 3 by the black heavy dashed lines (hardly visible for h=-0.075 in the upper right corner). We recognize that the essential feature, namely the energy gain due to the asymmetric deformations, is brought about quite far away from these bifurcations, and is thus determined by the shortest classical orbits in the central equatorial plane which is pushed aside to $z_0 \neq 0$ when the asymmetry sets in.

The white dashed lines in the right part of Fig. 3 give the loci of constant actions of the equatorial orbits at z_0, fixing their value at α=0. Note that the actions of all orbits in a given equatorial plane have the same deformation dependence. We see that the valley that leads from the isomer minimum over the outer fission barrier in the energetically most favorable way follows exactly the path of constant action of the leading classical orbits. This path is practically identical with that obtained in the quantum-mechanical shell-correction calculations. The essential result of our semiclassical investigation is therefore that the energetically most favorable asymmetric path to fission is governed by the principle of constant action of the leading classical orbits. This can be easily viewed already for the diameter orbit. In order to keep its length (and thus its action) constant on the way to fission, the nucleus must become left-right asymmetric (see the diameter lengths in the plots A and B on the left side of Fig. 5 below): along the symmetric path (α=0), the radius of the central equatorial plane would be squeezed even before the orbits have a chance to bifurcate and thereby to give way for longer orbits.

In Fig. 5, we show the same result as in the upper right of Fig. 3, but in a perspective view of a three-dimensional energy surface. On the left, we give the shapes of the cavity corresponding to the points A at the isomer minimum and the points B and C along the asymmetric fission barrier (see also the corresponding points in Fig. 3). Note that C lies beyond the bifurcation point and thus contains three planes of periodic orbits.

This concludes another example, demonstrating how a drastic rearrangement of the shape of a complex many-body system can be driven and described semiclassically by a few short periodic orbits. In Ref. [15] we have also pointed out that the classical phase-space dynamics of this system is partially chaotic, and that there is a close correspondence between the equatorial planes containing the leading classical orbits and those containing the wavefunction maxima of the single-particle states [32] responsible for the onset of the left-right asymmetry.

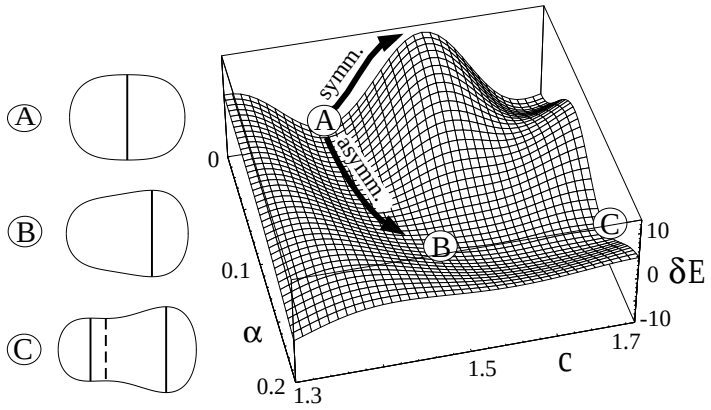

Figure 5: *Right*: $\delta E(c, \alpha)$ as in Fig. 3 (for h=0) in a perspective 3D plot. The arrows 'symmetric' and 'asymmetric' show two alternative fission paths. *Left*: shapes along the asymmetric fission path. The planes of the leading periodic orbits are shown by vertical lines (solid for stable and dashed for unstable orbits).

ACKNOWLEDGEMENTS

We acknowledge stimulating discussions with K. Arita, A. G. Magner and K. Matsuyanagi. This work was partially supported: *a*) by grant no. CHRX-CT94-0612 of the European Union, *b*) by the Studienstiftung des Deutschen Volkes and BASF-AG, and *c*) by Contract Nos. Ste 241/6-1 and Ste 241/7-2 of the Deutsche Forschungsgemeinschaft.

REFERENCES

[1] M. C. Gutzwiller, J. Math. Phys. **12**, 343 (1971).

[2] R. Balian and C. Bloch, Ann. Phys. (N. Y.) **69**, 76 (1972).

[3] V. M. Strutinsky and A. G. Magner, Sov. J. Part. Nucl. **7**, 138 (1976); V. M. Strutinsky, A. G. Magner, S. R. Ofengenden, T. Døssing, Z. Phys. **A 283**, 269 (1977).

[4] M. Brack and R. K. Bhaduri: *Semiclassical Physics* (Addison and Wesley, Reading, 1997).

[5] See, e.g., M. C. Gutzwiller: *Chaos in Classical and Quantum Mechanics* (Springer Verlag, New York, 1990); and *Chaos Focus Issue on Periodic Orbit Theory*, ed. P. Cvitanović: Chaos **2**, 1-158 (1992).

[6] V. M. Strutinsky, Nucl. Phys. **A 122**, 1 (1968); and earlier references quoted therein.

[7] H. Frisk, Nucl. Phys. **A 511**, 309 (1990).

[8] S. M. Reimann and M. Brack, Comp. Mat. Sci. **2**, 433 (1994).

[9] H. Nishioka, K. Hansen, B. R. Mottelson, Phys. Rev. **B 42**, 9377 (1990).

[10] J. Pedersen, S. Bjørnholm, J. Borggreen, K. Hansen, T. P. Martin, H. D. Rasmussen, Nature **353**, 733 (1991); S. Bjørnholm, these Proceedings.

[11] For a more detailed discussion, see also M. Brack, S. C. Creagh, P. Meier, S. M. Reimann, M. Seidl, in: *Large Clusters of Atoms and Molecules*, ed. by T. P. Martin (Kluwer, Dordrecht, 1996), p. 1.

[12] See also C. Bordas *et al.*, these Proceedings; for exhaustive Jellium-Kohn-Sham-LDA calculations of electronic supershells, see E. Koch and O. Gunnarsson, Phys. Rev. **B 54**, 5168 (1996).

[13] M. Persson, J. Pettersson, B. von Sydow, P. E. Lindelof, A. Kristensen, K. Berggreen, Phys. Rev. **B 52**, 8921 (1995).

[14] S. M. Reimann, M. Persson, P. E. Lindelof, M. Brack, Z. Phys. **B 101**, 377 (1996).

[15] M. Brack, S. M. Reimann M. Sieber, Phys. Rev. Lett. **79**, 1817 (1997).

[16] N. Bohr and J. A. Wheeler, Phys. Rev. **56**, 426 (1939).

[17] $x = E_c/2E_s$, where E_c and E_s are the Coulomb and surface energy, respectively, of the charged spherical liquid drop. When $x \geq 1$, the drop is unstable against fission. For further details see, e.g., L. Wilets: *Theories of nuclear fission* (Clarendon Press, Oxford, 1964).

[18] M. Brack, J. Damgård, A. S. Jensen, H. C. Pauli, V. M. Strutinsky, C. Y. Wong, Rev. Mod. Phys. **44**, 320 (1972).

[19] See M. Brack and P. Quentin, Nucl. Phys. **A 361**, 35 (1981), for numerical tests of the shell-correction method by Hartree-Fock calculations with realistic effective nucleon-nucleon interactions.

[20] S. G. Nilsson, C. F. Tsang, A. Sobiczewski, Z. Szymański, S. Wycech, C. Gustafsson, I.-L. Lamm, P. Möller, B. Nilsson, Nucl. Phys. **A 131**, 1 (1969).

[21] M. Bolsterli, E. O. Fiset, J. R. Nix, J. L. Norton, Phys. Rev. **C 5**, 1050 (1972); J. R. Nix, Ann. Rev. Nucl. Sci. **22**, 65 (1972).

[22] For a review on the physics of the 'double-humped fission barrier', see S. Bjørnholm and J. E. Lynn, Rev. Mod. Phys. **52**, 725 (1980).

[23] P. Möller and S. G. Nilsson, Phys. Lett. **31 B**, 283 (1970).

[24] H. C. Pauli, T. Ledergerber, M. Brack, Phys. Lett. **34B**, 264 (1971).

[25] See M. Brack, in: *Physics and Chemistry of Fission 1979*, (IAEA Vienna, 1980), Vol. I, p. 227, for a short review of fission barrier calculations and the role of various symmetries.

[26] See, e.g., J. Maruhn, W. Greiner, P. Lichtner, D. Drechsel, in: *Physics and Chemistry of Fission 1973* (IAEA Vienna, 1974), Vol. I, p. 569.

[27] A. G. Magner, S. N. Fedotkin, F. A. Ivanyuk, P. Meier, M. Brack, S. M. Reimann, H. Koizumi, Ann. Phys. (Leipzig) (1997), submitted.

[28] J. N. L. Connor, Mol. Phys. **26**, 1217 (1973).

[29] H. Schomerus and M. Sieber, J. Phys. **A 30**, 4537 (1997).

[30] K. Arita and K. Matsuyanagi, Nucl. Phys. **A 592**, 9 (1995).

[31] A. Sugita, K. Arita, K. Matsuyanagi, Kyoto University Preprint KUNS1431 (1997).

[32] C. Gustafsson, P. Möller, S. G. Nilsson, Phys. Lett. **34 B**, 349 (1971).